EFFECTS OF DIETARY CALORIE RESTRICTION OR EXERCISE ON THE PI3K AND RAS SIGNALING PATHWAYS IN THE SKIN OF MICE*

Linglin Xie‡, Yu Jiang‡, Ping Ouyang‡, Jie Chen‡, Hieu Doan‡, Betty Herndon¶, Jessica E. Sylvester‡, Ke Zhang§, Agostino Molteni¶, Marie Reichle¶, Rongqing Zhang‡, Mark D. Haub‡, Richard C. Baybutt‡, and Weiqun Wang‡

From the ‡Department of Human Nutrition, §Department of Statistics, Kansas State University, Manhattan, Kansas 66506 and the ¶School of Medicine, University of Missouri, Kansas City, MO 64108

Running title: Weight Loss and Cellular Signalling

Address correspondence to: Dr. Weiqun Wang, Department of Human Nutrition, Kansas State University, Manhattan, KS 66506, Tel. 785-532-0153; Fax. 785-532-3132; E-mail: wwang@ksu.edu

Weight control by exercise and dietary calorie restriction (DCR) has been associated with reduced cancer risk, but the underlying mechanisms are not well understood. This study was designed to compare the effects of weight loss by increasing physical activity or decreasing calorie intake on tumor promoter-induced Ras-MAPK and PI3K-Akt pathways. SENCAR mice were randomly assigned to one of the following five groups: ad libitum-fed sedentary control, ad libitum-fed exercise (AL+Exe), exercise but pair-fed at the amount as controls (PF+Exe), 20% DCR, and 20% DCR plus exercise (DCR+Exe). After 10-wks, body weight and body fat significantly decreased in the groups of DCR, DCR+Exe, and PF+Exe when compared with the controls. AL+Exe did not induce weight loss due to, at least in part, increased food intake. Plasma IGF-1 levels reduced significantly in DCR and DCR+Exe but not PF+Exe. The protein H-Ras and activated Ras-GTP significantly decreased in TPA-induced skin tissues of DCR-fed mice but not exercised mice. PI3K protein, phosphor-serine Akt, and p42/p44-MAPK were reduced, however, in both DCR and PF+Exe groups. Immunohistochemistry demonstrated that the significantly reduced H-Ras occurred in subcutaneous fat cells, while the reduced PI3K and PCNA took place only in epidermis. Plasma leptin decreased in PF+Exe, DCR, and DCR+Exe, while the caspase-3 activity increased in DCR+Exe only. Genomic microarray analysis further indicated that the expression of 34 genes relevant to PI3K and 31 genes to MAPK pathway were significantly regulated by either DCR or PF+Exe treatments. The reduced PI3K in PF+Exe mice was partially reversed by IGF-1 treatment. The overall results of this study demonstrated that DCR abrogated both Ras and PI3K signaling, which might inhibit TPA-induced proliferation and anti-apoptosis. Selective inhibition if PI3K by PF+Exe but not AL+Exe seems more attributable to the magnitude of the caloric deficit and/or body fat loss than diet vs. exercise comparison.

The National Health and Nutrition Examination Survey have indicated growing rates of obesity in American adults and overweight children over the past 20 years (1). Numerous prospective and case-control studies associated with weight control and physical activity estimate that excess body weight and sedentary life style account for about 39% of endometrial, 25% of kidney, 11% of colon, 9% of postmenopausal breast cancer, and 5% of total cancer incidence (2-3). It has been suggested that those 25% over normal weight have a 33% greater cancer risk than those who maintain ideal body weight (4). Therefore, for many individuals, it would be advisable to maintain weight within normal range to reduce their risk of cancer.

Overweight/obesity is recognized as a reflection of a positive energy state that results from either over-consumption of energy or low energy expenditure. There is ample evidence that weight control via decreasing calorie intake and/or increasing physical activity reduces cancer risk in animal models. For almost a century, dietary calorie restriction (DCR[1]) has been shown to inhibit the development of spontaneous, transplanted, chemically, and virally induced cancer in animal models (5-6). Many types of cancers, including mammary, liver, colon, skin, pancreas, bladder, and leukemia, have been shown

to be prevented by 20-40% DCR (7-8). Alternatively, exercise, an effective method for energy expenditure, has been also shown to reduce both the incidence of DMBA-induced colon tumors and the growth of transplanted tumors in rats (4, 9-10). Voluntary wheel running has been reported to inhibit UVB-induced skin carcinogenesis in hairless SKH-1 mice (11). The inhibition of tumor development by exercise is, however, modest if not combined with dietary restriction (12).

There are several hypotheses proposed to describe mechanisms by which weight control may reduce tumor development, including decreased oncogene expression, assisted DNA repair, scavenged reactive oxygen species, and altered levels of cancer-related hormones. Hormone alteration seems to be a critical factor for cancer prevention by weight control due to the significant role of hormones in regulating cellular growth. Previous researchers have found that the levels of insulin (13), IGF-1 (14-16) and leptin (14-17) decreased significantly in DCR-fed mice.

As a mitogen, IGF-1 is known to stimulate cell proliferation, inhibit apoptosis, and enhance angiogenesis (18). Chronically high levels of IGF-1 have been linked with an increased risk of developing breast (19-20), colon (21-22), and prostate (23) cancers in several case-control and prospective cohort studies. It has been suggested that the role of IGF-1 in mitogenesis is triggered through cellular signaling cascades leading to the activation of both mitogen activated protein kinase (MAPK) and phosphatidylinositol 3-kinase (PI3K) pathways (24).

The 12-*0*-tetradecanoylphorbol-13-acetate (TPA) is a cancer promoter that is topically applied to experimental mice in the skin cancer model (25-26). TPA can induce ras gene expression via Ras Guanyl Nucleotide- Releasing Protein (RasGRP). RasGRP is a family of guanyl nucleotide exchange factors and has been reported to be expressed in mouse epidermal keratinocytes in response to phorbol ester treatment (27-28). The activation of RasGRP by TPA is usually accompanied by subsequent Ras-mediated down-stream regulation, especially of the MAPK pathway (28).

Ras, a G-protein effector of IGF-1, is an important upstream regulator of the MAPK and PI3K pathways (29-30). Three ras genes have been identified in the mammalian genome: H-ras, K-ras and N-ras. They have similar structure and sequences and each codifies a monometric G protein of 21 KDa (29-30). H-ras is highly expressed in the skin and skeletal muscles, K-ras is mostly expressed in the colon and thymus, and N-ras is expressed in male germinal tissue and thymus (30). H-Ras and K-Ras are reported to be more responsive to the Raf-1/MAPK pathway. Ras becomes activated as a result of extracellular signals by the effect of its interaction with guanine exchange factors such as SOS. The combination of SOS and Ras stimulates GDP release. GTP then shifts from SOS to Ras (31). Activated GTP-bound Ras further initiates the MAPK cascade. Previous studies demonstrated that DCR treatment inhibited TPA-promoted skin carcinogenesis by reducing certain isoforms of PKC (32) down to the ERK pathway (33), and then repressing transcriptional regulation of AP-1 (34).

PI3K contains the p85 regulatory subunit (which has two SH2 Domains) and a 110 KD catalytic subunit (35). The PI3K's constitute a family of eight distinct PI3K isoforms divided into three classes according to their sequence homology and substrate preference. Class Ia, including p110α, p110β, and p110δ, is associated with a p85 regulatory subunit to form a heterodimeric complex. The p85 subunit has a binding site for both insulin and IGF-1 receptors. Thus, PI3Kα, β, and δ can be drawn the membrane and activated upon the autophosphorylation of tyrosine residues of IGF-1 receptor (36). In addition, Class Ia PI3K also can be activated by Ras-GTP via direct interaction with the catalytic subunit (37). Class Ib has only one member, p110γ, which is triggered by activated α, β, and γ heterotrimeric G-protein (37-38). PI3K down to Akt may modulate the function of numerous substrates involved in the regulation of cell survival, cell cycle progression, and cellular anti-apoptosis (39).

This study was designed to compare the effects of weight loss by DCR-fed or exercise-trained mice on Ras-MAPK and PI3K-Akt cascades. We provide novel evidence that these signaling pathways are potential targets by DCR and/or exercise for the inhibition of phorbol ester-induced skin tumor promotion. This is of particular interest because the key role of DCR- or exercise-induced weight control for these signal

pathways in cancer promotion by which IGF-1 and/or other hormones such as insulin and leptin may be involved is largely unknown. Better understanding the relationship between body weight status, endocrine hormone changes, and hormone-dependent signal pathway activation may lead to a novel approach for cancer prevention.

EXPERIMENTAL PROCEDURES

Animals and treatments: Female SENCAR mice were purchased from NIH (Frederick, MD) at 8 wks of age (30 ± 2 g). The SENCAR mouse was developed by a special breeding of CD-1 with skin tumor-sensitive mice for enhanced susceptibility to TPA-promoted skin carcinogenesis as originally described by Routwell (40). The averaged body weight was reduced (27.6 ± 2.8 g) after one-wk acclimation to new facility and diet change from rodent chow to AIN-93 purified diet. Mice were then randomly divided into one of the five groups: ad libitum sedentary (Control), ad libitum exercise (AL+Exe), Pair-fed plus exercise (PF+Exe), 20% DCR (DCR) and 20% DCR plus exercise (DCR+Exe). The PF+Exe group was paired-fed at the same amount as the control group. The mice were fed either a basal diet (AIN-93) or a 20% DCR diet for 12 wks. The 20% DCR diet was formulated and provided by Harlan Teklad (Madison, WI). Briefly, the DCR diet consisted of 20% less total calories from carbohydrates and fat in comparison with the basal AIN-93 diet, while the levels of protein and essential micronutrients were kept as same as the basal diet. The amount of food that each mouse consumed was recorded daily and averaged to determine the amount for the following week of the DCR and pair-fed consumption. A zero-grade adjustable-speed rodent treadmill (Boston Gears, Boston, MA) was used to exercise the mice. After a two-wk training period, mice performed treadmill exercise at 13.4 m/min for 60 min/d, 5 d/wk for 10 wks. Mice were housed individually in an environmentally controlled room maintained at 75 ± 1º and 80% relative humidity with a 12 h light/12 h dark cycle. To take into account the biological clocks of nocturnal rodents, the light cycle was adjusted for mice to run nighttime exercise. Body weights were recorded weekly. In the last two wks, some mice in PF+Exe group were received i.p. injection of either saline (sham) or IGF-1 (Novozymes GroPep, Australia) at 10 μg/g B.W. twice per week for IGF-1 treatment. The mice were fed until the last day, but exercise was stopped 24 hrs after the last bout. In the end of experiment, the dorsal skin of the mice was shaved and topically treated once with TPA at 3.2 nmol. Mice were sacrificed two hours after TPA treatment. The dorsal skin samples were snap-frozen in liquid nitrogen and kept at -70 ºC until further analyses.

Body fat analysis: Total body composition and bone mineral density were measured with a dual-energy X-ray absorptiometer scan (DXA) using small animal software (v5.6, Prodigy, Lunar-General Electric, Milwaukee, WI). Mice at the final week were anesthetized with sodium pentobarbitol prior to scanning. Body fat and bone mineral density were recorded from the DXA and presented as a percentage of the controls.

Assessment of plasma IGF-1 and leptin levels: Blood samples were obtained directly by decapitation and collected in heparin-coated tubes. Plasma was isolated by centrifugation at 1,000 g for 10 min at 4 ˚C. Total IGF-1 in plasma was extracted by Acid-ETOH method and was then measured by a RIA kit (Nichols Institute Diagnostic, San Clemente, CA). Plasma leptin levels were determined using a commercial murine leptin RIA kit (Linco Diagnosrics, St. Charles, MO).

Assessment of protein levels by western blotting: Western analysis was performed as described previously (41). Briefly, mouse skin tissues were homogenized in triton lysis buffer. Protein concentration was measured in the supernatant and 50 μg of whole cell protein was electrophoresed on 12% SDS polyacrylamide gel. The protein bands were transferred to a nitrocellulose membrane, and then the transferred bands of H-Ras (21 KDa), K-Ras (21 KDa), PI3K (110 KDa) and β-actin (internal control, 43 KDa) were respectively bound to their monoclonal antibodies purchased from Santa Cruz Biotechnology Inc. (Santa Cruz, CA). The monoclonal antibodies against IGF-1R beta (98 KDa) was provided by Upstate Inc. (Waltham, MA). Antibodies for p42/p44-MAPK (42/44 KDa), Akt (62 KDa), and p473-Akt (62 KDa) were provided by Cell Signaling Technology, Inc. (Danvers, MA). The bound proteins were treated with the appropriate HRP-conjugated secondary antibody (Santa Cruz Biotechnology Inc., Santa

Cruz, CA) and visualized by the FluorChem™ 8800 Advanced Imaging System (Alpha Innotech, San Leandro, CA). The expression levels of the proteins were qualified by a same imaging system. The relative density of the target band was normalized to the loading control β-actin and then expressed as a percentage of the controls.

Assessment of Activated Ras-GTP protein levels by pull down assay: Total activated Ras was determined by a pull down assay kit from Upstate Inc. (Waltham, MA). Briefly, the whole skin cell lysate was prepared in triton lysis buffer. The activated Ras in each 100 μg of cell lysate was then pelleted with 10 μL Raf-1 RBD agarose beads (Upstate Inc., Waltham, MA) at 12,000 g for 15 min. The pellet was washed in washing buffer three times. Pelleted samples were eluted in 2X loading buffer and boiled for 5 min. Samples were then loaded onto an 12% SDS-PAGE and transferred to a nitrocellulose membrane. The level of target protein was determined by anti-Ras $IgG_{2aκ,}$ specifically recognizing p21 H-, K- and N-Ras, followed by a goat anti-mouse-HRP conjugated IgG (Santa Cruz Biotechnology Inc., Santa Cruz, CA). The level of the activated GTP bound Ras was visualized by the FluorChem™ 8800 Advanced Imaging System as described before.

Assessment of local protein expression in skin tissue cells by immunohistochemistry: The flash-frozen dorsal skin tissues of mice were fixed in absolute ethanol overnight at -70 ºC, followed by 70% ethanol at 4 ºC, 50% ethanol at room temperature, and then rinsed with PBS before adding 10% formaldehyde. Then the skin tissues were set on edge in paraffin blocks to best demonstrate full skin thickness. Five micrometer sections of each skin sample were cut and mounted on positive precharged slides to ensure optimal adhesion. The sections were deparaffinized and rehydrated through 3 times of xylene incubation, twice of absolute ethanol, twice of 70% ethanol wash, and one PBS rinse. After endogenous peroxidase quenching (0.3% H_2O_2 in PBS for 20 min), antigens were retrieved by steaming at 95 ºC for 30 min with a commercial antigen retrieval solution (Dakocytomation, Carpinteria, CA). Following PBS washes, sections were incubated with 1/200 dilution of either one of the primary monoclonal antibodies that recognized mouse H-Ras (Santa Cruz Biotechnology, Santa Cruz, CA), PI3K (Santa Cruz Biotechnology, Santa Cruz, CA), PCNA (Invitrogen, Carlsbad, CA), caspase-3 (Sigma, St Louis, MO), and leptin (Affinity Bioreagents, Golden, CO), respectively. The incubation was kept for 2 hrs at room temperature in Tris-HCl buffer with 1% goat serum. Negative control slides were incubated with goat IgG only and without primary antibodies. Immunochemistry was performed using a biotin-streptavidin peroxidase technique (BioGenex, San Ramon, CA). Staining was developed with diaminobenzidine chromogen (BioGenex, San Ramon, CA). Staining density in epidermis, dermis, follicles, and subcutaneous fat of each section was blindly graded by the internal medicine residents using computer standards under guidance of a pathologist without knowledge of tissue treatment. The standards of staining intensity were respectively established at 400x by grading up to 40 cells in 5 unit increments from 3-5 mice per group. Data were statistically calculated and group difference scores with $p \leq 0.05$ were considered significant.

Caspase-3 activity assay: The activity of caspase-3 was measured using the fluorogenic substrate method (Kamiya Biomedical Company, Seattle, WA). Briefly, mouse skin tissue was homogenized in HEPES lysis buffer. Cell lysate at 500 μg of total protein content was incubated with the freshly prepared colorimetric substrate (*N*-acetyl-Asp-Glu-Val-Asp-7-amino-4-trifluoromethyl coumarin) at 5 μM, 37 ˚C for 30 min. The release of 7-amino-4-trifluoromethyl coumarin was then measured by a fluorescence spectrophotometer at 400 nm excitation and 505 nm emission.

Microarray analysis: Microarray analysis was performed by the Microarray Core of the Mental Retardation Research Center at the University of Kansas Medical Center. Four samples from four groups including the control, AL+Exe, PF+Exe, and DCR groups were analyzed as follows. Ten μg of total RNA was annealed with 100 pmol of T7(dT)24 at 70 ºC for 10 min. Then the annealed mRNA was reverse transcribed into cDNA using the Superscript Choice System kit (Invitrogen Corp., Carlsbad, CA). Biotinylated antisense cRNA was prepared using the Enzo BioArray High Yield RNA Labeling kit (Enzo Diagnostics, Farmingdale, NY). After purification of labeled cRNA using Rneasy RNA Purification Mini kit

(Qiagen), 20 μg biotin labeled cRNA was incubated in fragmentation buffer (40 mM Tris-Acetate, pH 8.1, 100 mM potassium acetate, 30 mM magnesium acetate) at 94 ºC for 35 min. The labeled cDNA then was applied to an Affymetrix oligonucleotide array, a GeneChip^{R} Mouse Genome 430 2.0 Array (Affymetrix, Santa Clara, CA) containing 39,000 transcripts with 45,101 probe sets. The genechip was hybridized, washed, and scanned using Affymetrix equipment and protocols (Affymetrix, Santa Clara, CA). Image data were quantified using genechip operating software 1.0 (GCOS 1.0). The detection calls of probe sets were determined using default settings (α1, 0.04; α2, 0.06; δ, 0.015; scale factor, 1.0; norm factor, 1.0). If a particular probe set was marked as "absent", the probe set was removed from further analysis. To detect the differentially expressed genes between treatment and control, a nonparametric bootstrap method (42) was used to compute the raw p-value for each gene. The eight chips from both the treatment groups and the control groups were re-sampled for 9,999 times with nonparametric bootstrapping, and t statistics of each gene was calculated for each re-sampling,. The raw p value for each gene was obtained by ranking the original t statistics value in the 9,999 re-sampling t statistics values. The differentially expressed genes were then determined by controlling the false-discovery rate (FDR) at the 1% level (43). From the total data pool, 48 genes relevant to IGF-1 signaling were found to be significantly impacted and reported in this study.

Gene expression confirmation by RT-PCR: RT-PCR reaction was carried out by using purified total RNA obtained as described above. The cDNA was synthesized by RT-PCR using one-step RT-PCR kit (Qiagen, Valeacia, CA). The primers are derived from published gene sequences as follows: MAPK1: sense primer 5'-TCT CCC GCA CAA AAA TAA GG-3', antisense primer 5'-TCG TCC AAC TCC ATG TCA AA-3'; H-ras: sense primer 5'-TGT TAC CAA CTG GGA CGA CA-3', antisense primer 5'-TCT CAG CTG TGG TGG TGA AG-3'; PI3Kca: sense primer 5'-TGT TTG CAA AGA AGC TGT GG-3', antisense primer 5'-TAT GAC CCA GAG GGA TTT CG-3'; IGFBP3: sense primer 5'-AAG TTC CAT CCA CTC CAT GC-3', antisense primer 5'-AGC TCT GCT TTC TGC CTT TG-3'; lepr: sense primer 5'-AGG CCC AGA CAT TTT TCC TT-3', antisense primer 5'-TCC TGG AGG ATC CTG ATG TC-3'; β-actin: sense primer 5'-TGT TAC CAA CTG GGA CGA CA-3', antisense primer 5'-TCT CAG CTG TGG TGG TGA AG-3'. Fifty μL of PCR reaction were run with a final concentration of 200 μM of dNTP mix, 1 x PCR buffer, 1 μM of each primer, and 1.0 U of Taq polymerase. Thermal cycling conditions, following an initial denaturation at 94 °C for 4 min, were as follows: 30 sec at 95 °C, annealing at 55 °C for 30 sec, and extension at 72 °C for 1 min. Then samples were incubated at 72 °C for 7 min. Amplified products at 8 μL were loaded and separated on a 1.5% agarose gel. The RT -PCR products were visualized under UV light by the FluorChem^{TM} 8800 Advanced Imaging System (Alpha Innotech, San Leandro, CA). The relative density of the target band was normalized to the loading control β-actin and then expressed as a percentage of the controls.

Statistic analysis: The overall effects of treatments on body weight, body fat, and IGF-1 levels were analyzed by one-way ANOVA, and then the least significant difference method (Fisher's LSD) was used to compare each of the treatment groups and the control group. Each set of comparisons for a given variable will be conducted at the overall 0.05 level of significance by applying Dunnett's adjustment. In the experiments of RT-PCR, activated Ras-GTP, western blotting, and immunohistochemistry, a complete randomized block design was used with each running gel as a block effect and analyzed by ANOVA and contrast analysis. All the statistical processes were carried out with SAS software.

RESULTS

Impact of DCR and exercise on Body weight and body fat: Figure 1A shows the effects of 20% DCR and exercise with or without diet intake limitation on body weight. Adult SENCAR mice in the control group gradually gained weight throughout the experimental period ($P < 0.01$, body weight at wk 12 vs. wk 1); however, mice at 20% DCR or 20% DCR plus exercise consistently lost weight during the experimental period ($P < 0.01$, body weight at wk 12 vs. wk 1). The PF+Exe mice had significantly lowered body weight at the end of the experiment when compared with the controls or AL+Exe group. By the end of the experiment, the mean weights of PF+Exe, DCR

and DCR+Exe mice were significantly lower than the controls. The weight of AL+Exe group was not significantly lower when compared with the sedentary counterparts, which might be, at least in part, due to their increased food intake (4.0 ± 0.2 g/day for control mice vs. 4.3 ± 0.4 g/day for AL+Exe mice). Consequently, percent body fat, as shown in Figure 1B, significantly decreased in PF+Exe, DCR, and DCR+Exe groups, but not AL+Exe group, when compared with the controls. No significant change of bone mineral density was found among groups (data not shown).

Impact on plasma IGF-1 and skin tissue IGF-1R levels: As shown in Figure 2A, plasma IGF-1 levels were significantly reduced in DCR and DCR+Exe groups when compared with control counterparts. Statistical analysis of the exercise factor with three exercise groups (AL+Exe, PF+Exe, and DCR+Exe) combined together demonstrated a significant decrease of IGF-1 levels in exercise-treated mice, but individual group alone did not show any significant change between exercise and control (data not shown). The protein levels of IGF-1R in skin tissues were not significantly different among groups (Figure 2B).

Impact on Ras-MAPK pathway: The protein levels of H-Ras, but not K-Ras, were significantly reduced in DCR and DCR+Exe mice. However, exercise did not show a significant effect (Figure 3A). The activated Ras-GTP, as measured by a pull down assay, was also significantly reduced in DCR and DCR+Exe mice, but not in exercise with ad libitum or pair-feeding mice in comparison with the control counterparts (Figure 3B). RT-PCR analysis indicated no significant alteration of H-ras gene expression among groups (Figure 3C). The p42/p44-MAPK levels were reduced significantly in DCR, DCR+Exe, and PF+Exe groups in comparison with the controls (Figure 3D).

Impact on PI3K-Akt pathway: The protein levels of PI3K significantly decreased in DCR, DCR+Exe, and PF+Exe mice when compared with the controls (Figure 4A). While the levels of Akt protein did not change, the levels of phosphor-serine Akt were significantly lower in DCR, DCR+Exe, and PF+Exe groups (Figure 4B).

Impact on local protein expression in skin tissues: Expression of PI3K, H-Ras, PCNA, leptin, and caspase-3 proteins in epidermis, dermis, follicles, and subcutaneous fat of the skin tissues was respectively assessed by immunohistochemistry. Representative images of PI3K, PCNA, and caspase-3 staining in epidermis and H-Ras staining in subcutaneous fat from acetone- or TPA-treated skin tissues were shown in Figure 5. In comparison with the acetone-treated control, TPA treatment significantly increased staining densities of PI3K, PCNA, and caspase-3 in epidermis as well as H-Ras in subcutaneous fat, respectively. However, TPA-enhanced densities of PI3K and PCNA in epidermis as well as H-Ras in subcutaneous fat significantly decreased in DCR and PF+Exe groups. There were no significant differences in AL+Exe group when compared with TPA-treated positive control only. There were no statistical differences of leptin (figure 6) and caspase-3 staining between treatment groups.

Effect on plasma leptin levels: In contrast to an unchanged local leptin production in the skin subcutaneous fat cells, plasma leptin levels in PF+Exe, DCR, and DCR+Exe groups but not AL+Exe group were significantly reduced in comparison with ad libitum-fed controls (Figure 6).

Effect on activated caspase-3 levels in skin tissues: Although the expression of caspase-3 protein in local skin cells as measured by immunohistochemistry was not changed, the caspase-3-like proteolytic activity in the cell lysates of skin tissues was potentially but insignificantly elevated following exercise- and/or DCR-treatments. A significant increase was found in DCR+Exe mice only when compared with that in the controls (Figure 7).

Effects of gene expression relevant to Ras and PI3K signaling pathways: By using Affymetrix microarray, we detected the effects of treatments on the expression of 39,000 transcripts with 45,101 probe sets in the skin tissues 2 hrs after TPA application. As shown in Table 1, 34 marker genes relevant to PI3K and 31 genes related to Ras-MAPK pathway were significantly changed. Eight of the marker genes relevant to PI3K and eleven genes to MAPK significantly decreased in DCR-fed mice, while five genes to PI3K and three to MAPK were considerably lowered in pair-fed but exercised mice. DCR-treatment also up-regulated expression of 15 genes related to PI3K and 14 genes to MAPK. In exercised mice with

pair feeding, 8 genes relevant to PI3K and 7 to MAPK significantly over-expressed when compared with the sedentary controls.

RT-PCR confirmation: The microarray data were further validated by using RT-PCR for five randomly selected genes in IGF-1-related categories. As shown in Figure 8 (MAPK1, PI3Kca, IGFBP3, and lepr) and Figure 3C (H-ras), the gene expression of MAPK1, PI3Kca, IGFBP3, and lepr was significantly decreased in DCR and DCR+Exe groups in comparison with the control group. PI3Kca expression was also reduced in PF+Exe group. The expression of H-ras was not significantly changed between experimental groups. The RT-PCR confirmation rate to the microrray data set, as estimated by using a Bayesian statistical method, is about 93.3%.

Impact on PI3K by IGF-1 treatment: The mice in PF+Exe group were received i.p. injection with either saline (sham) or IGF-1 at 10 μg/g B.W. twice per wk in the last two weeks. As shown in Figure 9, the levels of expression in skin samples were significantly reduced in PF+Exe when compared to the controls. However, the reduced PI3K in PF+Exe group was partially reversed by IGF-1 injection.

DISCUSSION

The major foci of this study are to elucidate the potential mechanisms of cancer prevention by weight loss and to compare the impact between DCR and physical activity. By using a combined weight control protocol with DCR and exercise components in an epidermal carcinogenesis-sensitive mouse strain, we assessed the effects of DCR and exercise on body weight, body fat, and plasma IGF-1 levels. The mechanistic impact of body weight reduction by DCR or exercise on Ras-MAPK and PI3K-Akt signal pathways was further assessed in cancer promoter phorbol ester-promoted skin tissues.

Previous data have shown DCR at 10% does not affect DMBA-induced tumor incidence in rats, but reduces tumor size (44). At 20% DCR, tumor incidence fell by one third, and tumor size was reduced similar to that of 10% DCR (44). The 30% and 40% DCR reduced both tumor incidence and size even more (45). However, certain undesired side effects occurred at the level greater than 30% DCR (46). In this study, we chose 20% DCR and introduced treadmill exercise for the first time to compare the impact of weight control between decreasing calorie intake and increasing energy expenditure.

As expected, we found that body weight significantly decreased with 20% DCR, which corresponded to a decrease of body fat and plasma IGF-1 levels. In contrast to DCR treatment, the impact of treadmill exercise demonstrated a modest but intricate result for weight maintenance. Exercise alone with ad libitum feeding was not sufficient to decrease body weight due to, at least in part, the corresponding increase in dietary intake. However, the dietary energy increase in AL+Exe might not necessarily match the treadmill exercise-induced energy expenditure, since the energy expenditure could have been altered due to the changed spontaneous activity in the cage and/or resting energy metabolism, etc. If the food intake of the exercised mice was limited by pair-feeding with sedentary counterpart, then body weight and body fat were significantly reduced. Plasma levels of IGF-1 seemed lowered, but were not significantly reduced by exercise. It should be noted that the caloric deficit was not matched between the exercise and DCR interventions, and thus the results should be interpreted accordingly. The estimated increase in energy expenditure by treadmill exercise at a moderate intensity in this study (13.4 m/min for 60 min/d, 5 d/wk for 10 wks) seems much lower than the 20% reduction in dietary calorie intake. Particularly, the lack of an exercise effect in AL+Exe mice on the body weight/fat, IGF-1, and various signaling markers might be in part due to the insufficient energy expenditure of exercise. In comparison with DCR, therefore, a partial inhibition of signaling pathways by PF+Exe and no inhibition by AL+Exe may be more attributable to the magnitude of the calorie deficit than the dietary calorie intake vs. exercise comparison.

Although negative energy balance is a fundamental cause of weight loss, the body weight in the DCR group combined with exercise treatment did not show any additive decrease when compared with DCR alone. Clearly, the role of physical activity in total energy expenditure and energy homeostasis is complicated. Badman and Flier recently summarized that the total energy expenditure should consist of physical activity, adaptive thermogenesis, and obligatory energy

expenditure (46). It should be noted that both calorie restriction and exercise have been found to suppress plasma thyroid hormones (47-48). It is well known that thyroid hormones enhance energy conservation and resist loss of weight. It is possible that the combination of calorie restriction and exercise could suppress thyroid hormone action to a greater extent than calorie restriction alone and therefore explain the similar weight loss for both types of treatments.

The signaling transduction pathways promoted by TPA in skin carcinogenesis are well characterized. Briefly, TPA activates PKC-Raf-MAPK signal transduction pathways and then promotes proliferation. Previous studies have demonstrated that DCR inhibited skin carcinogenesis by suppressing TPA-induced AP-1 transcriptional activation via blocking PKC-Raf-ERK signal (32-34). Our current data provide significant novel information that the reduction of circulating IGF-1 levels may induce an abrogated IGF-1-dependent signaling, and thereby co-inhibit TPA-induced cancer promotion.

While the basal levels of most signaling events tested in acetone-treated TPA-free skin tissues were not significantly impacted by DCR intervention (33-34), we found that 20% DCR for 10 wks significantly inhibited TPA-promoted Ras-MAPK and PI3K-Akt pathways as well as proliferative marker PCNA. The finding that H-Ras protein levels and activated Ras levels are depressed by DCR is in agreement with the skin tissue specificity of Ras. It is interesting that immunohistochemistry staining indicates that the decrease of H-Ras expression occurred in subcutaneous fat cells, but not in epidermis. To our knowledge, this is the first study to report that DCR reduces TPA-induced H-Ras expression in subcutaneous fat cells. It is not clear how a reduction of H-Ras in subcutaneous fat may impact skin carcinogenesis that originally develops from epidermis. The role of subcutaneous fat on malignant melanoma, however, has been suggested via tumor-stroma interaction required during metastases (49) or early micrometastases (50). Recent data also suggest that adipocytes not only respond to hormonal signals, but also produce hormone-like factors such as adiponectin or pro-inflammatory adipocytokines that may enhance oncological risk (51-52). Therefore, we further measured the local production of leptin in skin subcutaneous fat cells and found that was not significantly changed by either diet or exercise treatment. It is interesting that a significant decrease of plasma leptin levels was found in PF+Exe, DCR, and DCR+Exe groups, suggesting other resources of circulating leptin such as abdominal fat. The earlier study by Michna et al. (11) showed 31-42% lower weight of parametrial fat pads in the wheel running mice when compared to non-runners. Although the runners did not significantly lose body weight due to increased food intake, they had a significant inhibition against UVB-induced skin carcinogenesis (11). Therefore, a dietary consideration by pair-feeding in the exercised mice might be not necessary for cancer prevention. The lack of altered skin signaling events in AL+Exe group in this study might be related to absence of body fat loss, which is consistent with the results in the PF+Exe group. Follow-up studies in the Wang laboratory are on-going to look for the association of reduced body fat with plasma leptin levels as well as lipidomics profiling in exercised mice.

In contrast to DCR that suppressed both Ras-MAPK and PI3K-Akt pathways in TPA-treated skin tissues, treadmill exercise with pair-feeding selectively reduced only the PI3K-Akt pathway. The activation of the PI3K-Akt pathway, as marked by p110 PI3K protein levels, activated phosphor Akt, p110 PI3K protein expression in epidermis, and their corresponding gene expression, was significantly lower in DCR, DCR+Exe, and PF+Exe groups in comparison with the controls. The selective inhibition of PI3K-Akt signaling in phorbol ester-promoted skin samples by exercise with pair-feeding may be associated with anti-apoptosis. Depressing this signaling pathway may increase apoptosis and thus protect against cancer development (53-54). We further measured the levels of caspase-3 as an apoptosis marker and found that the caspase-3-like proteolytic activity did potentially increase but not significant following physical activity or DCR treatments. A significant increase in caspase-3 activity by the combination of DCR and exercise together may further support an involvement of an apoptosis-mediated mechanism.

It is well known that not only IGF-1 but also some other hormones or growth factors such as insulin and leptin could activate both PI3K-Akt

and Ras-MAPK signal cascades. It is interesting that IGF-1 injection partially abolished the suppression of PI3K in pair-fed and exercised mice, suggesting a requirement of IGF-1 reduction on down-expression of p110 PI3K protein observed in those mice. We still cannot exclude the involvement of other hormones that have been found to be significantly changed in response to weight control (13, 14-17). Future studies to elucidate the individual or the combined effects of IGF-1 with other changed hormones on PI3K and Ras signaling in weight controlled mice appear to be warranted.

By using our established strategies to control body weight, we measured the genomic gene expression in TPA-promoted skin tissues and compared the TPA-induced gene expression profiles between exercise and DCR treatments. Of the 39,000 transcripts with 45,101 probe sets measured, we identified 559 genes that showed at least 1.5-fold significant change by DCR and/or exercise treatments in comparison with the controls. Of these 559 genes, 411 genes were altered by DCR, 110 genes were changed by AL+Exe, and 67 genes were changed by PF+Exe. By using gene ontology annotation, we identified the altered genes in 21 major biological processes including cell growth, cell maintenance, cell communication, DNA binding, transcription factor, and transcription activity categories. A list of all the genes that significantly changed by either DCR or exercise treatment with all the gene ontology categories has been published separately (55). The results of 34 genes relevant to PI3K pathway and 31 genes related to MAPK pathway were selected to report here. Much of the altered genes were consistent with the results of protein and active protein measurements, which showed the treatments of DCR and exercise with pair-feeding suppressed the expression of 16 genes relevant to PI3K or MAPK pathways. However, some of the marker genes were unexpectedly over-expressed. The precise reason underlying this discrepancy is unknown. Considering that the microarray data were detected at one time point, a time course of gene expression in response to TPA treatments and the corresponding proteomic data may help to explain any potential inconsistencies. An alternative explanation for the unexpected gene over-expression observed from microarray results may be associated with potential crosstalk by other undetected pathways. This could also explain the data by which exercise with pair feeding did not affect Ras protein and activity levels, but attenuated downstream MAPK activity and then TPA-induced PCNA staining.

Taken together as illustrated in Figure 10, the well-known cancer prevention by DCR treatment, therefore, appears to be a consequence of the reduced Ras/MAPK in subcutaneous fat and PI3K/Akt signaling in epidermis, and results in decreased sensitivity to TPA stimuli in skin tissues leading to suppressed proliferation and expressed potential apoptosis. Exercise with limited dietary intake, but not exercise alone, induced a decrease of PI3K/Akt signaling in epidermis. These reductions seem to be related to the decrease of circulating IGF-1 levels, but an involvement of other hormones such as insulin and leptin might not be excluded.

In conclusion, this study demonstrated for the first time that a successful strategy to control body weight via decreasing calorie intake or increasing physical activity led to the reduction of corresponded Ras-MAPK and/or PI3K-Akt pathways. DCR induced substantial weight loss and significantly decreased IGF-1 levels for a comprehensive inhibition of both MAPK and PI3K pathways. DCR alone was as effective as DCR+Exe, indicating that DCR, independent of exercise, is a potent inhibitor for tumor-promoting pathways. Exercise with pair-feeding but not exercise alone, however, only selectively restrained the PI3K pathway, which seemed more attributable to the magnitude of the caloric deficit and/or body fat loss than diet vs. exercise comparison.

REFERENCES

1. Hedley, A. A., Ogden, C. L., Johnson, C. L., Carroll, M. D., Curtin, L. R., and Flegal, K. M. (2004) *JAMA* **291,** 2847-2850
2. Bergstrom, A., Pisani, P., Tenet, V., Wolk, A., and Adami, H. O. (2001) *Interl. J. Cancer* **91,** 421-430
3. International Agency for Research on Cancer. (2002) *IARC Handbooks of Cancer Prevention* (Vol. 6, Lyon, IARC)
4. Kritchevsky, D. (2003) *J. Nutr.* **133**(11 Suppl. 1), 3827S-3829S
5. Weindruch, R., and Walford, R. L. (1988) *The retardation of aging and disease by dietary restriction* (Springfield, IL)
6. Hursting, S. D., Perkins, S. N., and Phang, J. M. (1994) *Proc. Natl. Acad. Sci. USA* **91,** 7036-7040
7. Pollard, M., Luckert, P. H., and Pan, G. Y. (1984) Cancer Treat. Rep. 68, 405-408
8. Roebuck, B. D., Yager, J. D., Jr., and Longnecker, D. S. (1981) *Cancer Res.* **41,** 888-893
9. Michna, L., Wagner, G. C., Lou, Y. R., Xie, J. G., Peng, Q. Y., Lin, Y., Carlson, K., Shih, W. J., Conney, A. H., Lu, Y. P. (2006) *Carcinogenesis.* (electronic publication ahead of print)
10. Rusch, H. P., and Kline, B. E. (1944) *Cancer Res.* **4,** 116-118
11. Michna, L., Wagner, G. C., Lou, Y., Xie, J., Peng, Q., Lin, Y., Carlson, K., Shih, W. J., Conney, A. H., and Lu, Y. (2006) *Carcinogenesis* **27**, 2108-2115
12. Garrow, J. S., and Summerbell, C. D. (1995) *Eur. J. Clin. Nutr.* **49,** 1-10
13. Dean, D. J., Gazdag, A. C., Wetter, T. J., and Cartee, G. D. (1998) *Aging* **10,** 303-307
14. Mai, V., Colbert, L. H., Berrigan, D., Perkins, S. N., Pfeiffer, R., Lavigne, J. A., Lanza, E., Haines, D. C., Schatzkin, A., and Hursting, S. D. (2003) *Cancer Res.* **63**, 1752-1755
15. Zhu, Z., Jiang, W., and Thompson, H. J. (2002) *Mol. Carconog.* **35,** 51-56
16. Hursting, S. D., Switzer, B. R., French, J. E., and Kari, F. W. (1993) *Cancer Res.* **53,** 2750-2757
17. Figlewicz, D. P., Higgins, M. S., Ng-Evans, S. B., and Havel, P. J. (2001) *Physiol. Behav.* **73,** 229-234
18. Werner, H., and Le Roith, D. (2000) *Cell. Mol. Life Sci.* **57,** 932-942
19. Palmqvist, R., Hallmans, G., Rinaldi, S., Biessy, C., Stenling, R., Riboli, E., and Kaaks, R. (2002) *Gut* **50,** 642-646
20. Wu, Y., Cui, K., Miyoshi, K., Hennighausen, L., Green, J. E., Setser, J., LeRoith, D., and Yakar, S. (2003) *Cancer Res.* **63**, 4384-4388
21. Hankinson, S. E., Willett, W. C., Colditz, G. A., Hunter, D. J., Michaud, D. S., Deroo, B., Rosner, B., Speizer, F. E., and Pollak, M. (1998) *Lancet* **351,** 1393-1396
22. Wu, Y., Yakar, S., Zhao, L., Hennighausen, L., and LeRoith, D. (2002) *Cancer Res.* **62**, 1030-1035
23. Mukherjee, P., Sotnikov, A. V., Mangian, H. J., Zhou, J. R., Visek, W. J., and Clinton, S. K. (1999) *J. Natl. Cancer Inst.* **91,** 512-523
24. Benito, M., Valverde, A. M., and Lorenzo, M. (1996) *Int. J. Biochem. Cell. Biol.* **28,** 499-510
25. Boutwell, R. K. (1974) *CRC Crit. Rev. Toxicol.* **2,** 419-443
26. DiGiovanni, J. (1992) *Pharmacol. Ther.* **54,** 63-128
27. Ebinu, J. O., Bottorff, D. A., Chan, E. Y., Stang, S. L., Dunn, R. J., and Stone, J. C. (1998) *Science* **280,** 1082-1086
28. Rambaratsingh, R. A., Stone, J. C., Blumberg, P. M., and Lorenzo, P. S. (2003) *J. Biol. Chem.* **278,** 52792-52801
29. Mariano, B. (1987) *Ann. Rev. Biochem.* **56,** 779-827
30. Lowy, D. R., and Willumsen, B. M. (1993) *Annu. Rev. Biochem.* **62,** 851-891
31. Boriack-Sjodin, P. A., Margarit, M. S., Bar-Sagi, D., and Kuiyan, J. (1998) *Nature* **394,** 337-343
32. Birt, D. F., Duysen, E., Wang, W., and Yaktine, A. (2001) *Cancer Epidemiol. Biomark Prev.* **10,** 679-85

33. Liu, Y., Wang, W., Hawley, J., and Birt, D. F. (2002) *Cancer Epidemiol. Biomark Prev.* **11,** 299-304
34. Przybyszewski, J., Yaktine, A. L., Duysen, E., Blackwood, D., Wang, W., Au, A. & Birt, D. F. (2001) *Carcinogenesis* **22,** 1421-1427
35. Fresno Vara, J. A., Casado, E., de Castro, J., Cejas, P., Belda-Iniesta, C., and Gonzalez-Baron, M. (2004) *Cancer Treat. Rev.* **30,** 193-204
36. Dent, P., Yacoub, A., Contessa, J., Caron, R., Amorino, G., Valerie, K., Hagan, M. P., Grant, S., and Schmidt-Ullrich, R. (2003) *Radiat. Res.* **159,** 283-300
37. Downward, J. (1998) *Curr. Opin. Genet. Dev.* **8,** 49-54
38. Kishimoto, H., Hamada, K., Saunders, M., Backman, S., Sasaki, T., Nakano, T., Mak, T. W., and Suzuki, A. (2003) *Cell. Struct. Funct.* **28,** 11-21
39. West, K. A., Castillo, S. S., and Dennis, P. A. (2002) *Drug Resist. Updat.* **5,** 234-248
40. Boutwell, R. K. (1964) *Progr. Exptl. Tumor Res.* **4**, 207-250
41. Taylor, S. J., Resnick, R. J., and Shalloway, D. (2001) *Methods Enzymol.* 333, 333-342
42. Efron, B., and Tibshirani, R. J. (1986) *Stat. Sci.* 1, 54-77
43. Benjamini, Y., and Hochberg, T. (1995*) J. R. Stat. Soc.* B57, 289-300
44. Klurfeld, D. M., Welch, D. B., Davis, M. J., and Kritchevsky, D. (1989) *J. Nutr.* **119,** 286–289
45. Kritchevsky, D. (1995) *Eur. J. Cancer Prev.* **4,** 445-51
46. Badman, M. K., and Flier, J. S. (2005) *Science* **307,** 1909-1914
47. Roth, G. S., Handy, A. M., Mattison, J. A., Tilmont, E. M., Ingram, D. K., and Lane, M. A. (2002) *Horm. Metab. Res.* **34,** 378-382
48. Mastorakos, G., and Pavlatou, M. (2005) *Horm. Metab. Res.* **37,** 577-584
49. Smolle, J., Hofmann-Wellenhof, R., Woltsche-Kahr, I., Haas, J. And Kerl, H. (1995) *Am. J. Dermatopathol*. **17**, 555-559
50. Proebstle, T. M., Huber, R., and Sterry, W. (1996) *Eur. J. Cancer* **32A**, 1664-1667
51. Berstein, L. M. (2005) *Adv. Gerontol.* **16,** 51-64
52. Miyazawa-Hoshimoto, S., Takahashi, K., Bujo, H., Hashimoto, N., Yagui, K., and Saito, Y. (2005) *Am. J. Physiol. Endocrinol. Metab.* **288,** E1128-E1136
53. Schaeffer, H. J., and Weber, M. J. (1999) *Mol. Cell. Biol.* **19,** 2435-2444
54. Hagan, H., and Sharrocks, A. D. (2003) *EMBO Rep.* **3,** 415-419
55. Lu, J., Xie, L., Sylvester, J., Wang, J, Bai, J., Baybutt, R., and Wang, W. (2007) *Exp. Biol. Med.* **232**, 473-480

* This work was supported in part by an Innovative Research Grant from the Terry C. Johnson Center for Basic Cancer Research, Kansas State University (to W.W.), NIH COBRE Award P20 RR15563 and Kansas State matching support (to W.W.), and NIH R01 CA106397 (to W.W.). This is a journal contribution #04-354-J by the Kansas Agricultural Experiment Station, Kansas State University.
Address correspondence to: Weiqun Wang, Department of Human Nutrition, Kansas State University, Manhattan, KS 66506, Tel. 785-532-0153; Fax. 785-532-3132; E-mail: wwang@ksu.edu
[1] The abbreviations used are**:** AL, ad libitum; DXA, dual-energy X-ray absorptiometry; PF, pair-fed; DCR, dietary calorie restriction; ERK, extracellular signal-regulated protein kinase; PBS: phosphate buffer saline solution; PKC, protein kinase C; TPA, 12-*0*-tetradecanoylphorbol-13-acetate; RIA, radioimmunoassay.

Table 1: Impact of weight control via dietary calorie restriction (DCR) or treadmill exercise with pare feeding (PF+Exe) on the expression of 48 genes up regulated (↑) or down regulated (↓) that are relevant to MAPK (+) and/or PI3K (+) pathways.

Accession Number	Symbol	PI3K	MAPK	DCR	PF+Exe
BB248138	Dmtf1	+	+	↓	
BG143376	Prkcz	+	+	↓	
AI451506	Rps6kb1	+	+	↓	↓
BB389420	Prkca	+	+	↓	
BB141769	Braf		+	↓	
AW553456	Map2k2		+	↓	
AV377656	Map3k5		+	↓	
BG070504	Map4k4		+	↓	
NM_011949	Mapk1		+	↓	
BI414398	Mapk3		+	↓	
BB018528	Nras		+	↓	↓
NM_008113	Arhgdig	+		↓	↓
AI528567	Pik3ca	+		↓	↓
NM_008841	Pik3r2	+		↓	
BM207149	Rps6kc1	+		↓	↓
AI649005	Igfbp3	+	+	↑	
BB345784	Irs1	+	+	↑	
BM124366	Lepr	+	+	↑	
NM_008860	Prkcz	+	+	↑	
BB370469	Map3k12		+	↑	
BE948629	Map3k3		+	↑	↑
BQ174980	Mapkbp1		+	↑	
AI987929	Ndrg1		+	↑	
NM_008681	Ndrl		+	↑	↑
BB354696	Rasgrp1		+	↑	
BF019839	Akt1s1	+		↑	
BM222798	Arhgap15	+		↑	
BB749468	Arhgap17	+		↑	
NM_133962	Arhgef18	+		↑	
NM_017367	Ccni	+		↑	
BI872151	Ccnt2	+		↑	
NM_010585	Itpr1	+		↑	
NM_008713	Nos3	+		↑	↑

BC017537	Pik3r4	+		↑	
BG069493	Rgnef	+		↑	↑
BG972377	Tnfrsf21	+		↑	
NM_031880	Tnk1	+		↑	↑
NM_010517	Igfbp4	+	+		↓
BM201230	Map3k9		+		↑
BB469472	Mapkapk3		+		↑
NM_025846	Rras2		+		↑
AI324972	Sp4		+		↑
AI746342	Stat6		+		↑
BF018155	Pik3cb	+			↑
BG076163	Crebbp	+			↑
NM_019923	Itpr2	+			↑
BB752796	LOC547217	+			↑
BE914497	Pfkl	+			↑

Figure Legend:

Figure 1. Effect of DCR and exercise on body weight and percent body fat. Female SENCAR mice at 9 wks of age (27.6 ± 2.8 g) were divided into five groups: ad libitum sedentary (Control), ad libitum exercise (AL+Exe), Pair-fed plus exercise (PF+Exe), 20% DCR (DCR), and 20% DCR plus exercise (DCR+Exe).). The mice were fed either a basal diet (AIN-93) or a 20% DCR diet for 12 wks. The PF+Exe group was paired-fed at the same amount as the ad libitum sedentary group. Mice performed treadmill exercise at 13.4 m/min for 60 min/d, 5 d/wk for 10 wks. A: Body weights of the mice at the final week were significantly reduced in DCR, DCR+Exe, and PF+Exe groups. Results are means of n = 8-12 per group. Means with different letters differ significantly ($P \leq 0.05$). B: Body composition of the mice at the final week was measured by DXA scan. Percent body fat significantly decreased in DCR, DCR+Exe, and PF+Exe groups. Results are mean ± SE (n = 8-12, *$P \leq 0.05$ vs. the controls).

Figure 2. Effect of DCR and exercise on plasma IGF-1 and skin tissue IGF-1R levels. Total IGF-1 levels in plasma were measured by a RIA kit. A: The plasma IGF-1 levels in DCR and DCR+Exe groups were significantly reduced in comparison with ad libitum-fed controls. B: The protein levels of IGF-1R in skin tissues as measured by western blotting were not significantly changed between groups. The relative expression level of IGF-1R was normalized to the level of loading control β-actin and then expressed as a ratio to the controls. Results are mean ± SE (n = 8-12, *$P \leq 0.05$ vs. the controls).

Figure 3. Effect of DCR and exercise on IGF-1-dependent Ras-MAPK Pathway. A: Levels of H-Ras (white bar), but not K-Ras(black bar), significantly reduced in DCR and DCR+Exe groups. B: Activated Ras measured by pull down assay as described under "Experimental Procedure" significantly decreased in DCR and DCR+Exe groups when compared to the controls. C: H-ras gene expression measured by RT-PCR as described under "Experimental Procedures" was not significantly altered between groups. D: Levels of p42/p44-MAPK in PF+Exe, DCR, and DCR+Exe groups were significantly reduced when compared to the controls. The densities of the appropriate band were quantified by the FluorChem™ 8800 Advanced Imaging System. The relative density of the target band was normalized to the loading control β-actin and then expressed as a ratio to the controls. Results are presented as mean±SE (n = 7, *$P \leq 0.05$ vs. the controls).

Figure 4. Effect of DCR and exercise on IGF-1-dependent PI3K-Akt Pathway: A: Levels of p110 PI3K protein were significantly reduced in PF+Exe, DCR, and DCR+Exe groups. B: p-Akt(Ser473), but not Akt, significantly decreased in PF+Exe, DCR, and DCR+Exe groups when compared to the controls. The expression levels of the proteins were quantified by the FluorChem™ 8800 Advanced Imaging System. The relative density of the target band was normalized to the loading control β-actin and then expressed as a ratio to the controls. Results are presented as mean±SE (n = 7, *$P \leq 0.05$ vs. the controls).

Figure 5. Detection of protein expression of PI3K, H-Ras, PCNA, and caspase-3 by immunohistochemistry staining. Representative histological skin sections with immunohistochemical staining as described under "Experimental Procedures" for PI3K, PCNA, and caspase-3 in epidermis and H-Ras in subcutaneous fat in acetone-treated control (A) and those TPA-treated mice from control (B), DCR (C), PF+Exe (D), and AL+Exe (E) are shown. The arrows indicate representative staining of a target protein in epidermis and subcutaneous fat cells, respectively. TPA significantly enhanced the densities of PI3K, PCNA, and caspase-3 in epidermis as well as H-Ras in subcutaneous fat cells compared with acetone-treated controls. The TPA-induced densities of PI3K, PCNA, and H-Ras but not caspase-3 staining significantly decreased in DCR and PF+Exe groups when compared with the TPA-treated controls ($P \leq 0.05$, n=3-5).

Figure 6. Effect of DCR and exercise on plasma leptin and local leptin production in skin subcutaneous fat. Plasma leptin levels as measured by a RIA kit in DCR and DCR+Exe groups were significantly reduced in comparison with ad libitum-fed controls. The production of local leptin in subcutaneous fat cells as measured by immunohistochemistry staining was not significantly changed between treatment groups. Results are mean ± SE (n = 6-9, *$P \leq 0.05$ vs. the controls).

Figure 7: Effect of DCR and exercise on proteolytic activity of caspase-3. The cell lysates of skin tissues taken 2 hrs after TPA application were incubated with fluorogenic caspase-3 substrate as described under "Experimental Procedures". A significant increase in caspase-3-like proteolytic activity in DCR+Exe mice was found when compared with the controls (n=3-4, *$P \leq 0.05$ vs. the controls).

Figure 8: Confirmation of microarray data by RT-PCR. Five genes were randomly chosen from cancer-related categories and their expression pattern in comparison with the microarray data was validated by RT-PCR as showed in Figure 8 and Figure 3c, respectively. Identical results were obtained with MAPK1, PI3Kca, IGFBP3, and lepr genes but nor H-ras gene that down-expressed significantly in DCR and DCR+Exe groups. The gene expression of PI3K was also significantly reduced in PF+Exe group.

Figure 9. Impact on p110-PI3K protein levels by IGF-1 treatment: As mentioned above in Figure 1, the PF+Exe mice were paired-fed at the same amount as the ad libitum sedentary group and performed treadmill exercise at 13.4 m/min for 60 min/d, 5 d/wk for 10 wks. In the last two weeks, they were i.p. injected with saline (sham) or IGF-1 at 10 μg/g B.W. twice per wk. Levels of p110-PI3K protein as measured by Western blotting were significantly reduced in PF+Exe when compared to the controls. However, the reduced PI3K in PF+Exe group was partially reversed by IGF-1 injection. Results are mean ± SE (n = 5-7). Bars with different alphabetical letters differ significantly, $P \leq 0.05$.

Figure 10. Hypothesized weight control-induced inhibitory crosstalk between IGF-1-dependent and TPA-promoted signaling pathways. Dietary calorie restriction reduced circulated IGF-1 levels and then suppressed TPA-activated Ras-MAPK and PI3K-Akt pathways in both protein and gene expression levels. Exercise with pair-feeding reduced the PI3K-Akt pathway and MAPK-p42/44, but exercise with ad libitum feeding did not affect body weight, plasma IGF-1, or any of the signaling pathways that were studied.

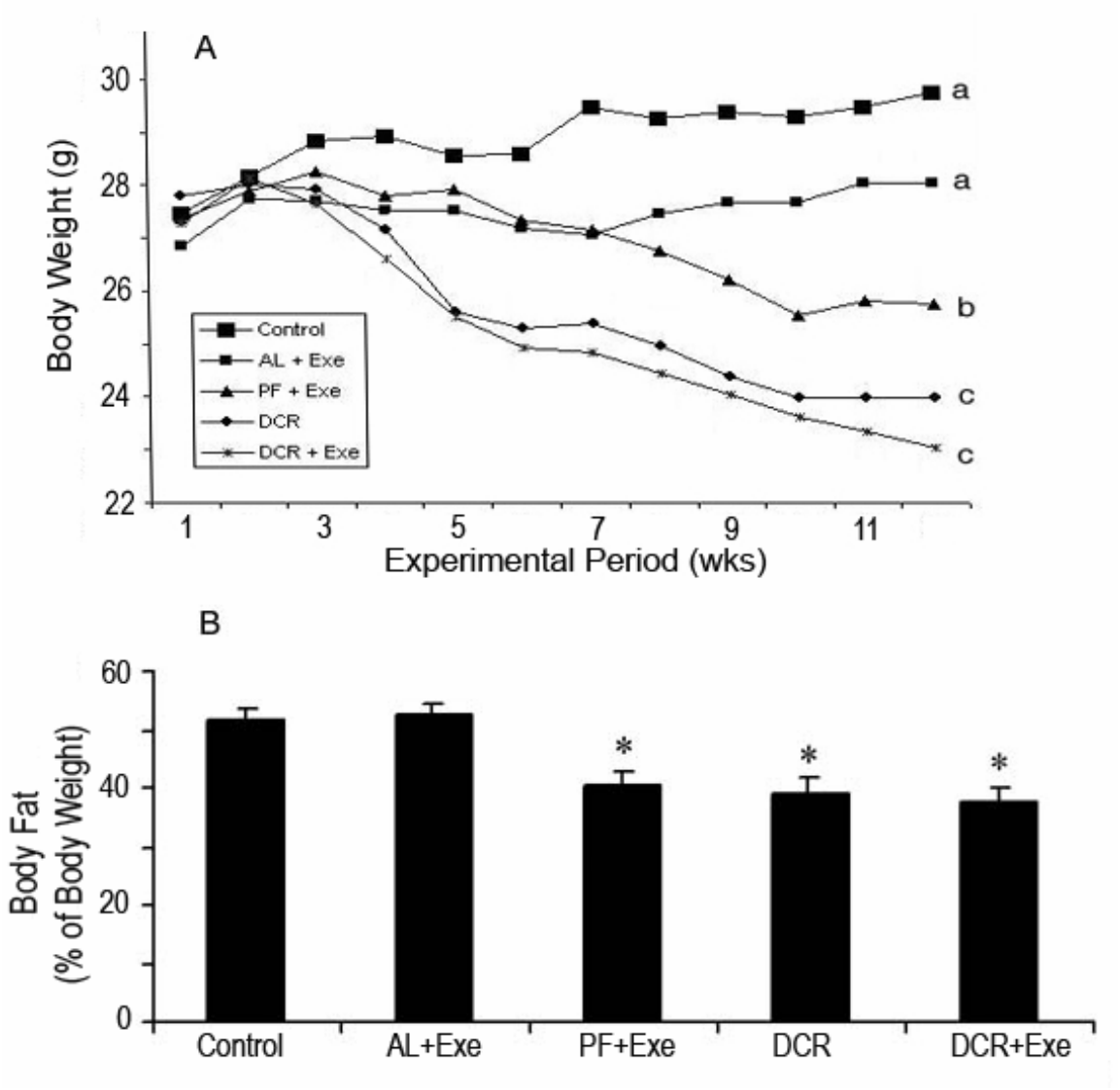
A
Body Weight (g)
30
28
26
24
22
1
3
5
7
9
11
Experimental Period (wks)
Control
AL + Exe
PF + Exe
DCR
DCR + Exe
a
a
b
c
c
B
Body Fat
(% of Body Weight)
60
40
20
0
Control
AL+Exe
PF+Exe
DCR
DCR+Exe
*
*
*

Figure 1

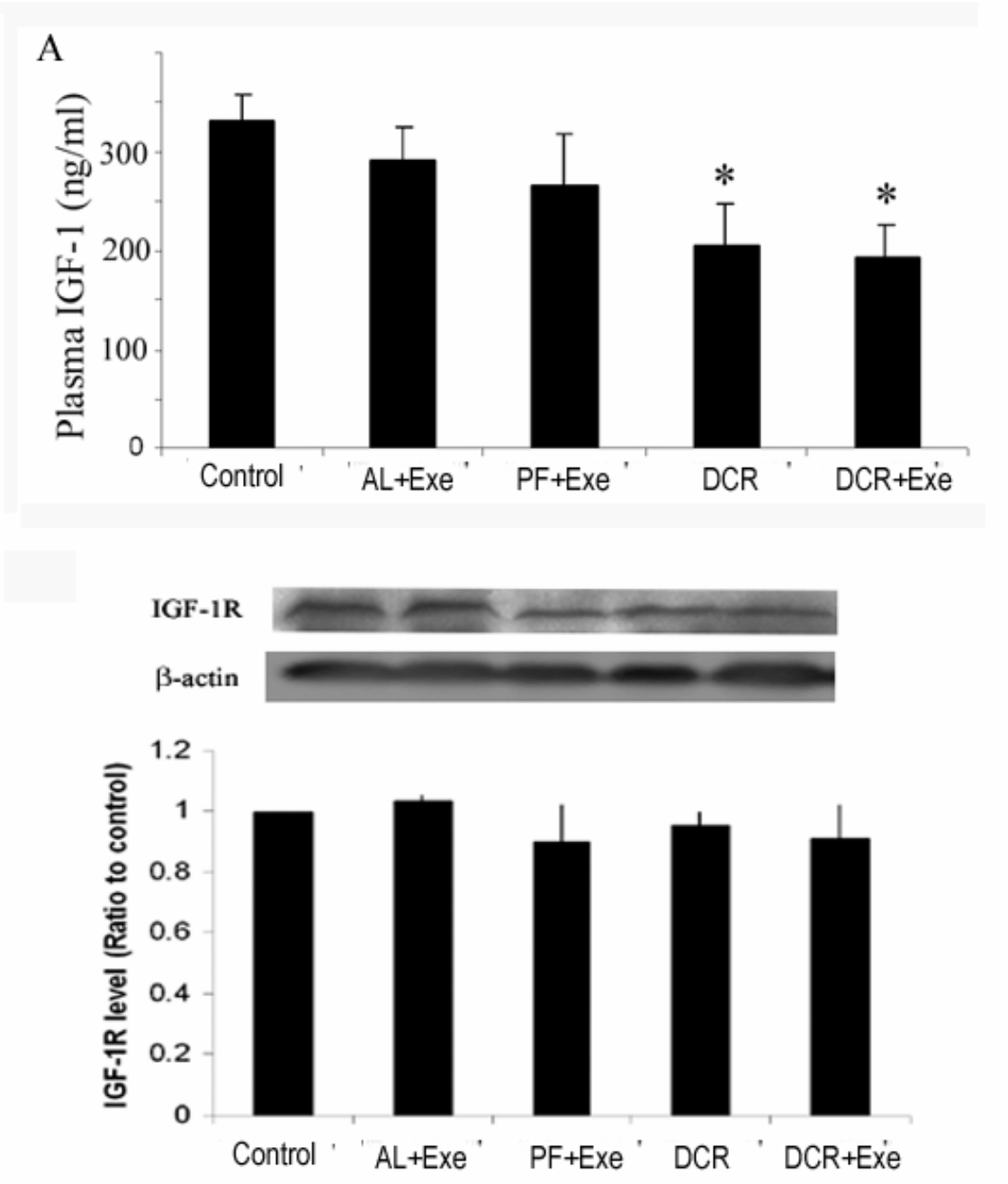
A
Plasma IGF-1 (ng/ml)
300
200
100
0
*
*
Control
AL+Exe
PF+Exe
DCR
DCR+Exe
IGF-1R
β-actin
IGF-1R level (Ratio to control)
1.2
1
0.8
0.6
0.4
0.2
0
Control
AL+Exe
PF+Exe
DCR
DCR+Exe

Figure 2

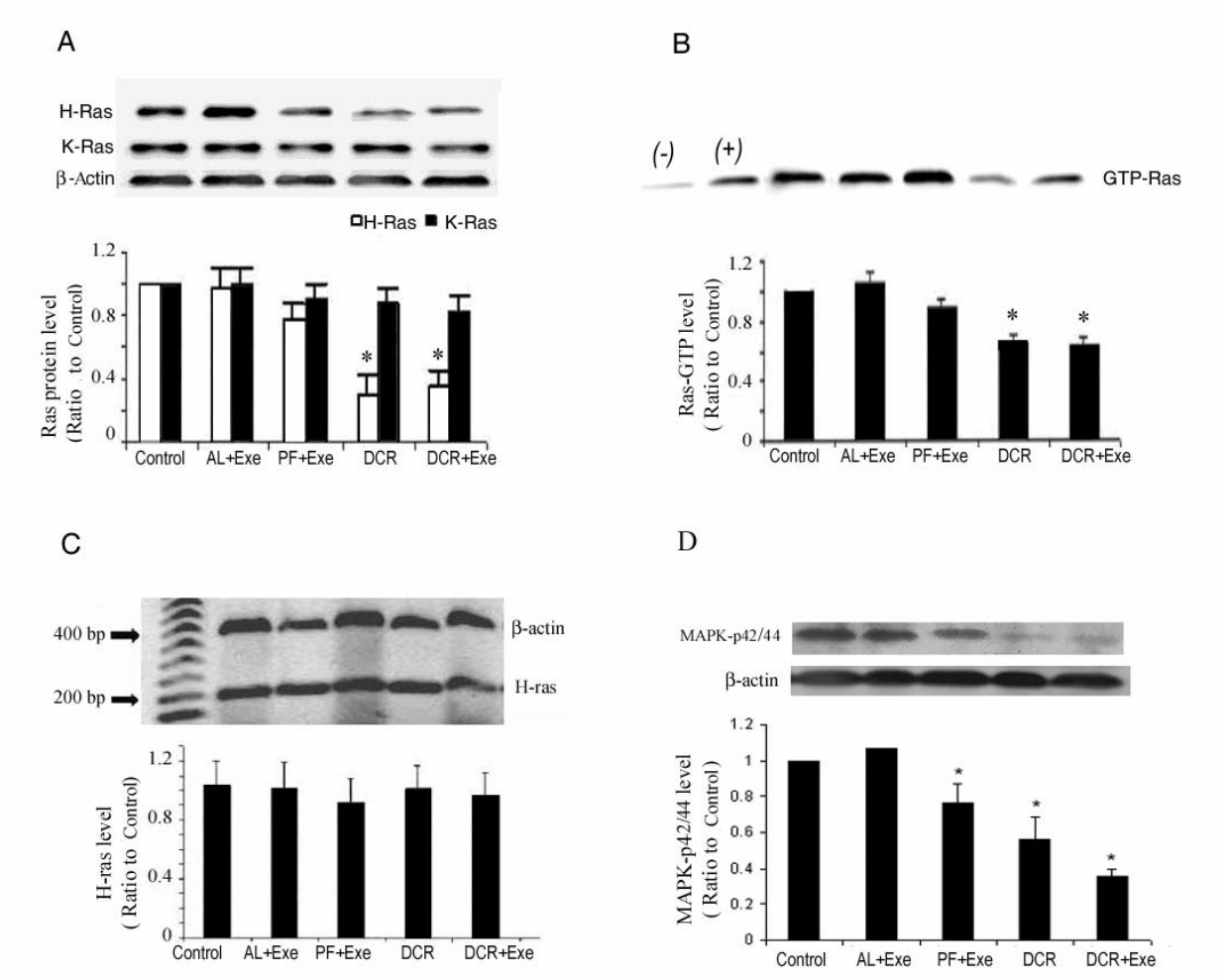
A
H-Ras
K-Ras
β-Actin
H-Ras K-Ras
Ras protein level (Ratio to Control)
1.2
0.8
0.4
0
Control AL+Exe PF+Exe DCR DCR+Exe
B
(-) (+)
GTP-Ras
Ras-GTP level (Ratio to Control)
1.2
0.8
0.4
0
Control AL+Exe PF+Exe DCR DCR+Exe
C
400 bp
200 bp
β-actin
H-ras
H-ras level (Ratio to Control)
1.2
0.8
0.4
0
Control AL+Exe PF+Exe DCR DCR+Exe
D
MAPK-p42/44
β-actin
MAPK-p42/44 level (Ratio to Control)
1.2
1
0.8
0.6
0.4
0.2
0
Control AL+Exe PF+Exe DCR DCR+Exe

Figure 3

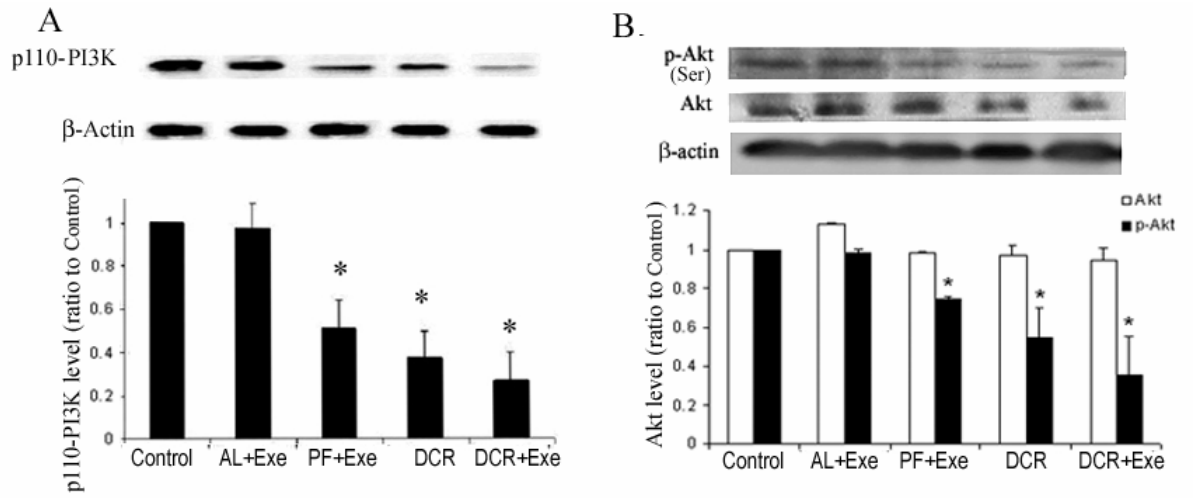
A
p110-PI3K
β-Actin
p110-PI3K level (ratio to Control)
0
0.2
0.4
0.6
0.8
1
Control
AL+Exe
PF+Exe
DCR
DCR+Exe
B
p-Akt (Ser)
Akt
β-actin
Akt
p-Akt
Akt level (ratio to Control)
0
0.2
0.4
0.6
0.8
1
1.2
Control
AL+Exe
PF+Exe
DCR
DCR+Exe

Figure 4

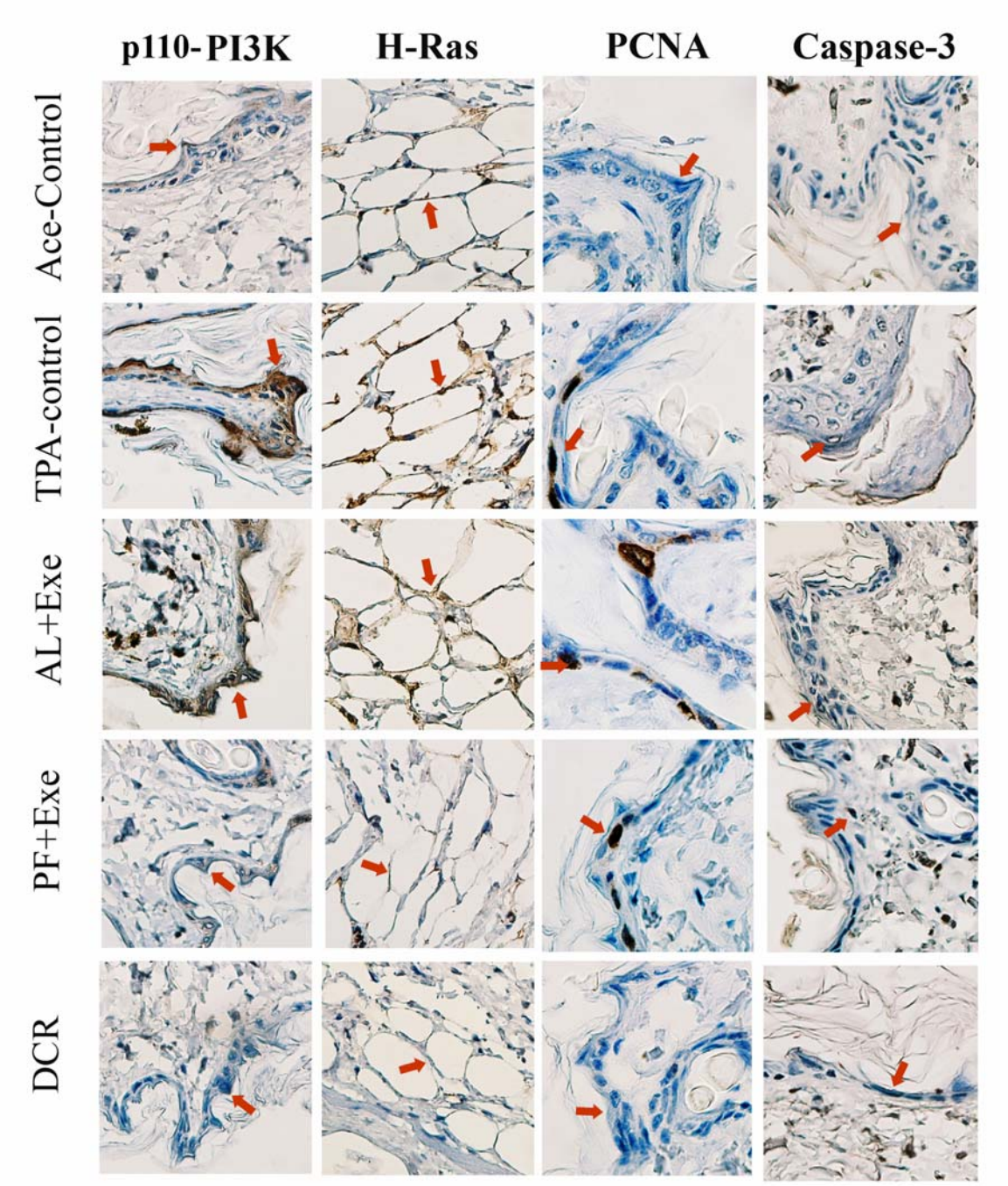
p110-PI3K
H-Ras
PCNA
Caspase-3
Ace-Control
TPA-control
AL+Exe
PF+Exe
DCR

Figure 5

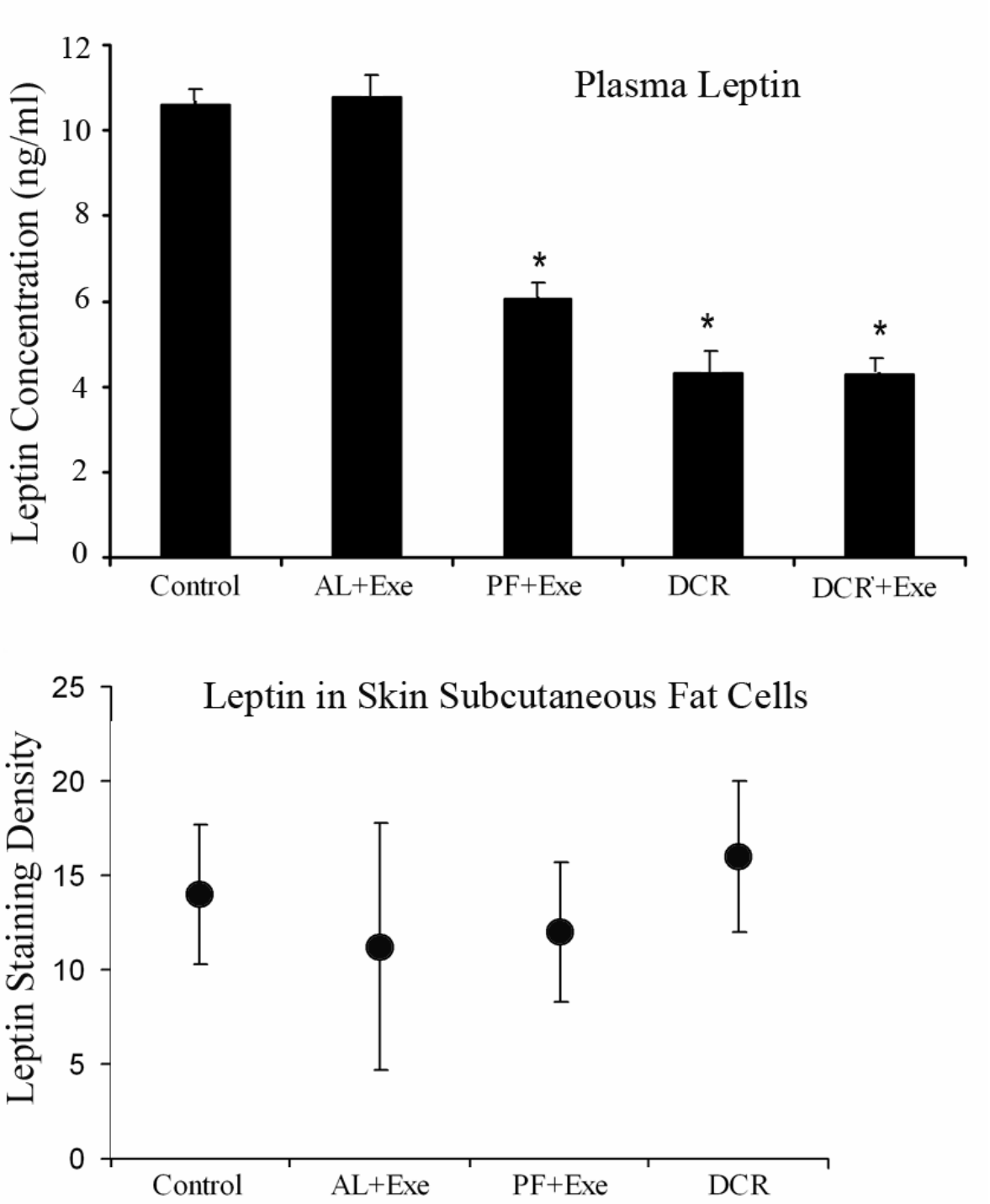
Plasma Leptin
Leptin Concentration (ng/ml)
12
10
8
6
4
2
0
*
*
*
Control
AL+Exe
PF+Exe
DCR
DCR'+Exe
Leptin in Skin Subcutaneous Fat Cells
Leptin Staining Density
25
20
15
10
5
0
Control
AL+Exe
PF+Exe
DCR

Figure 6

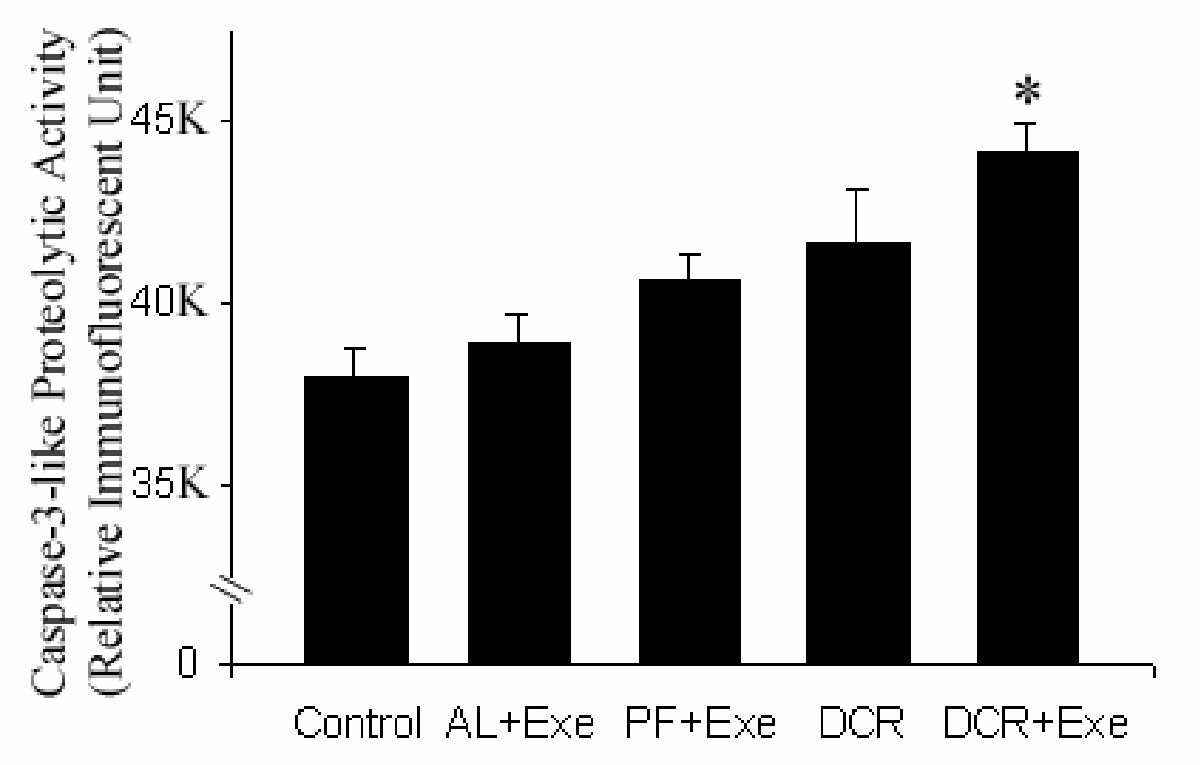
Caspase-3-like Proteolytic Activity
(Relative Immunofluorescent Unit)
45K
40K
35K
0
*
Control
AL+Exe
PF+Exe
DCR
DCR+Exe

Figure 7

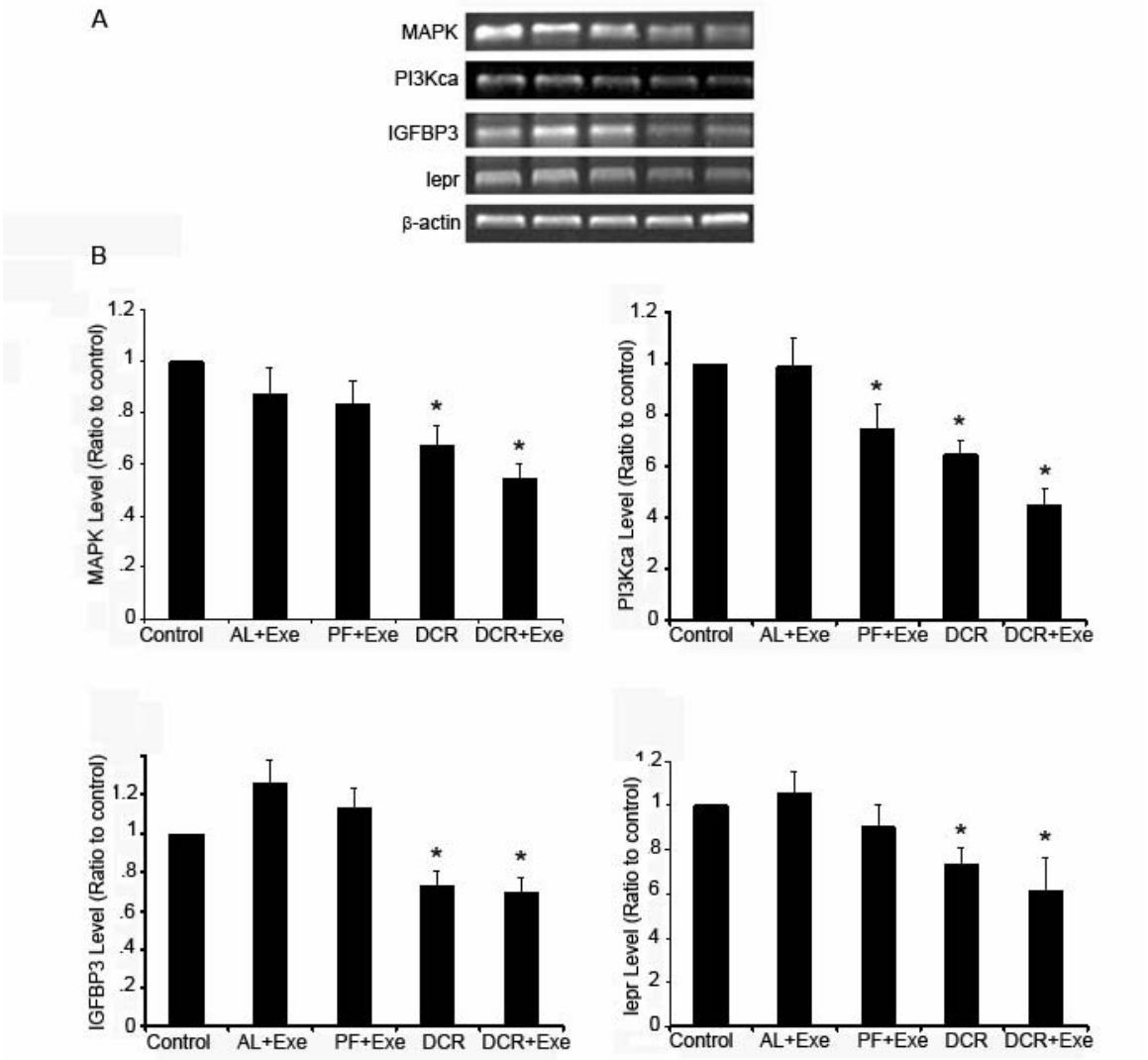
A
MAPK
PI3Kca
IGFBP3
Iepr
β-actin
B
MAPK Level (Ratio to control)
PI3Kca Level (Ratio to control)
IGFBP3 Level (Ratio to control)
Iepr Level (Ratio to control)
Control
AL+Exe
PF+Exe
DCR
DCR+Exe

Figure 8

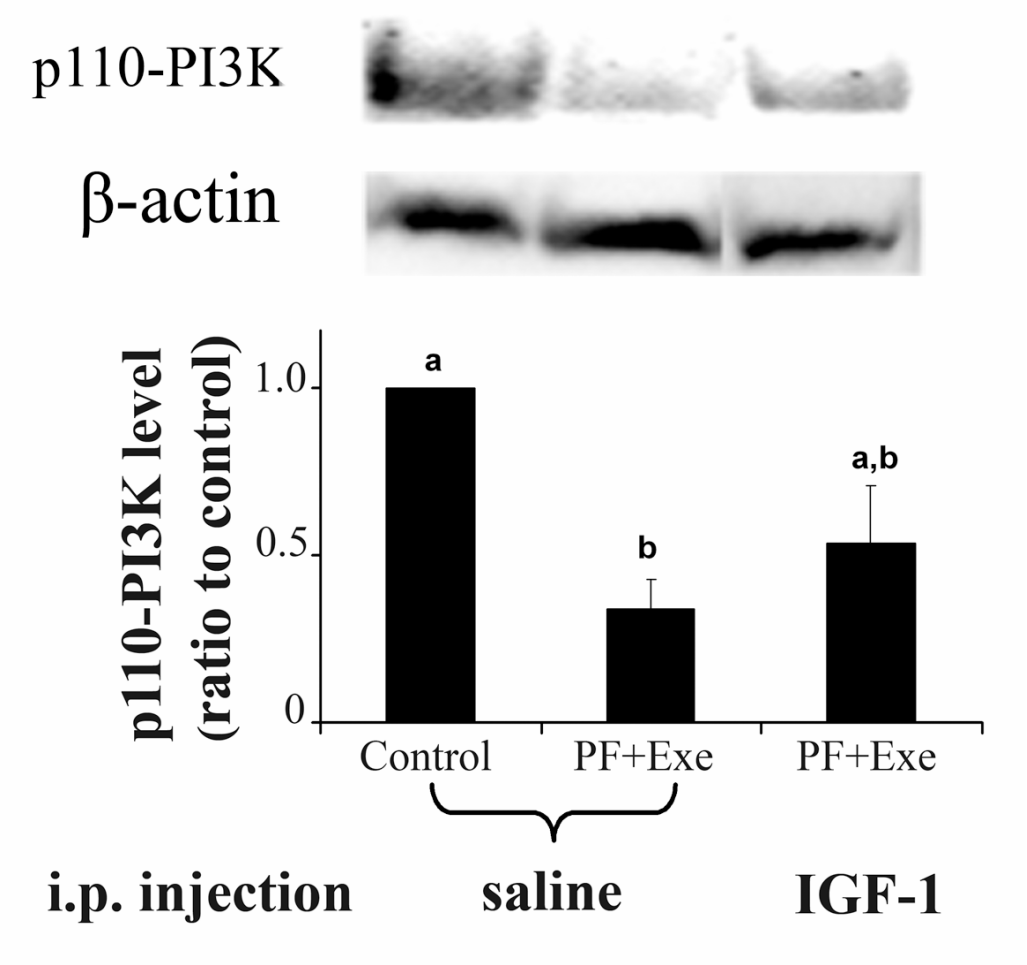
p110-PI3K
β-actin
p110-PI3K level
(ratio to control)
1.0
0.5
0
a
b
a,b
Control
PF+Exe
PF+Exe
i.p. injection
saline
IGF-1

Figure 9

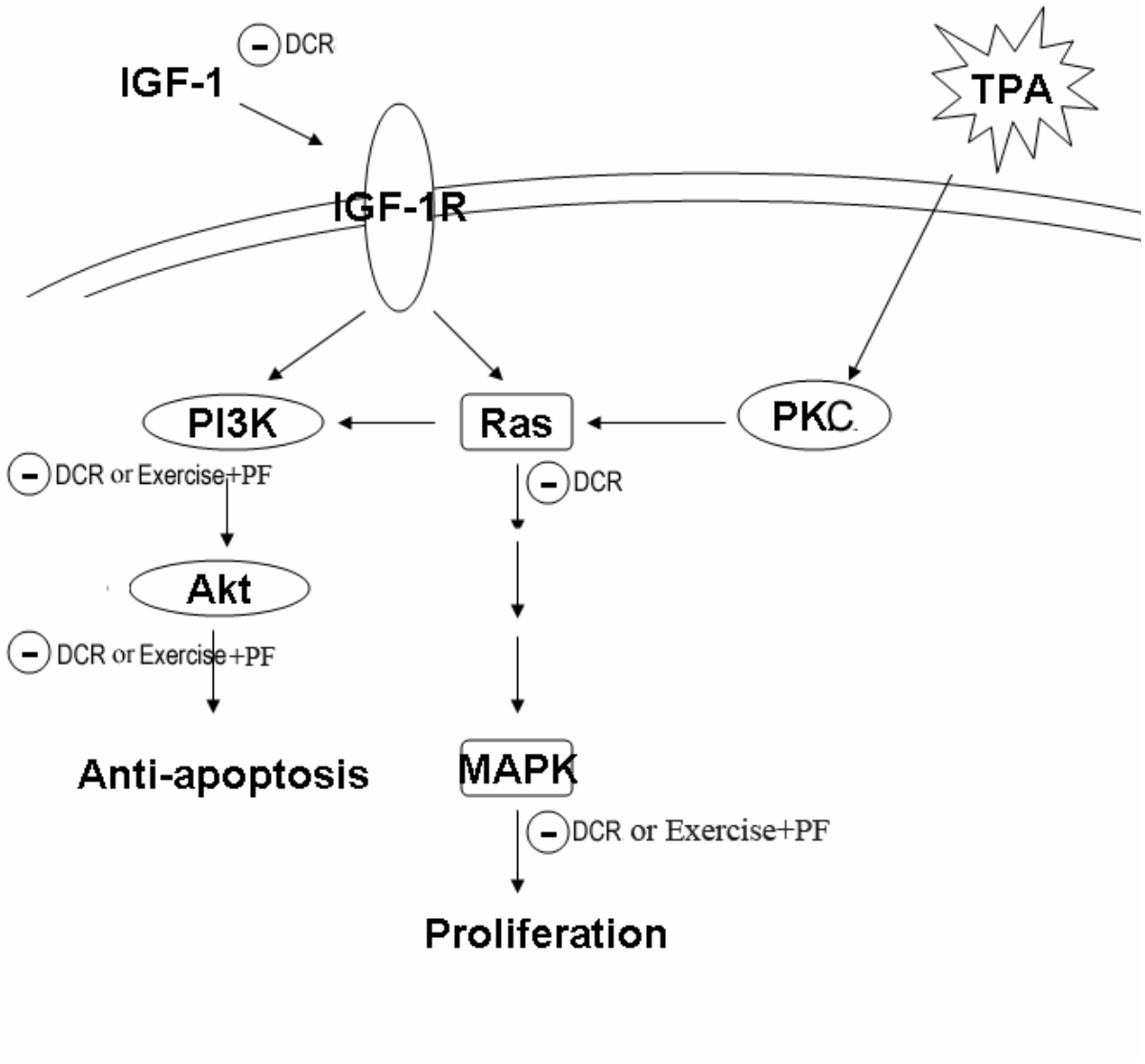
DCR
IGF-1
TPA
IGF-1R
PI3K
Ras
PKC
DCR or Exercise+PF
DCR
Akt
DCR or Exercise+PF
Anti-apoptosis
MAPK
DCR or Exercise+PF
Proliferation

Figure 10